Cancer Cell
Article

Distinct Thresholds Govern Myc's Biological Output In Vivo

Daniel J. Murphy,[1,4,5] Melissa R. Junttila,[1,4] Laurent Pouyet,[1] Anthony Karnezis,[2] Ksenya Shchors,[1] Duyen A. Bui,[1,6] Lamorna Brown-Swigart,[1] Leisa Johnson,[3] and Gerard I. Evan[1,2,*]
[1]Department of Pathology
[2]Helen Diller Family Comprehensive Cancer Center
University of California, San Francisco, San Francisco, CA 94143, USA
[3]Genentech, Inc., South San Francisco, CA 94080, USA
[4]These authors contributed equally to this work
[5]Present address: Lehrstuhl für Physiologische Chemie II, Am Hubland, 97074 Würzburg, Germany
[6]Present address: Department of Cell Biology, Harvard Medical School, Boston, MA 02115, USA
*Correspondence: gevan@cc.ucsf.edu
DOI 10.1016/j.ccr.2008.10.018

SUMMARY

Deregulated Myc triggers a variety of intrinsic tumor suppressor programs that serve to restrain Myc's oncogenic potential. Since Myc activity is also required for normal cell proliferation, activation of intrinsic tumor suppression must be triggered only when Myc signaling is oncogenic. However, how cells discriminate between normal and oncogenic Myc is unknown. Here we show that distinct threshold levels of Myc govern its output in vivo: low levels of deregulated Myc are competent to drive ectopic proliferation of somatic cells and oncogenesis, but activation of the apoptotic and ARF/p53 intrinsic tumor surveillance pathways requires Myc overexpression. The requirement to keep activated oncogenes at a low level to avoid engaging tumor suppression is likely an important selective pressure governing the early stages of tumor microevolution.

INTRODUCTION

The Myc oncoprotein is a pleiotropic transcription factor of the basic helix-loop-helix-leucine zipper family with the essential role of engaging and coordinating expression of the diverse genes necessary for efficient and orderly proliferation of somatic cells. In normal cells, both mRNA and protein expression of c-Myc are low and continuously dependent on mitogen signaling (Liu and Levens, 2006; Rabbitts et al., 1985; Ramsay et al., 1984). In most human cancers, by contrast, Myc expression is deregulated and/or elevated. Sometimes this is due to alterations in the *myc* gene itself that disrupt its normal regulation (e.g., chromosomal translocation, retrovirus integration, or gene amplification), increase *myc* mRNA or Myc protein stability, or abrogate Myc autorepression (reviewed by Nesbit et al., 1999; Popescu and Zimonjic, 2002; Spencer and Groudine, 1991). In most tumors, however, the c-*myc* gene appears normal, and its elevated and persistent activity appears to be due to its relentless induction by upstream oncoproteins, such as oncogenic kinases, Ras, or the Wnt/β-catenin pathway.

The extent to which Myc deregulation versus Myc overexpression contributes to Myc oncogenic activity is unclear. Increasing Myc levels often correlate with the more advanced and aggressive variants of tumors, suggesting that overexpression plays some part in Myc-driven oncogenesis. Moreover, since overexpression drives novel interactions between Myc and low-affinity promoter elements, some have suggested that Myc's oncogenic actions arise from precocious recruitment of novel genes (Fernandez et al., 2003). On the other hand, deregulation of Myc without overexpression is sufficient to obviate the dependency of normal cell proliferation on mitogens and to block the response of cycling cells to antiproliferative cues. This is most

SIGNIFICANCE

Cancers are prevented by the activation of intrinsic tumor suppressor programs that either fix the damage in cells or ensure that the damaged cells cannot propagate. Cancers can only arise once these tumor suppressor pathways are abrogated. Importantly, activation of such tumor suppressor pathways must be restricted only to oncogenic, not normal, growth signals. Using an in vivo model of Myc-induced tumorigenesis in which Myc function is deregulated without concomitant overexpression, we show that tumor surveillance programs are triggered specifically by Myc overexpression, not deregulation. Nonetheless, low-level deregulated Myc remains potently oncogenic. These observations identify a mechanism by which the tumor suppressor defense mechanisms can be circumvented, with implications for our understanding of early-stage neoplasia.

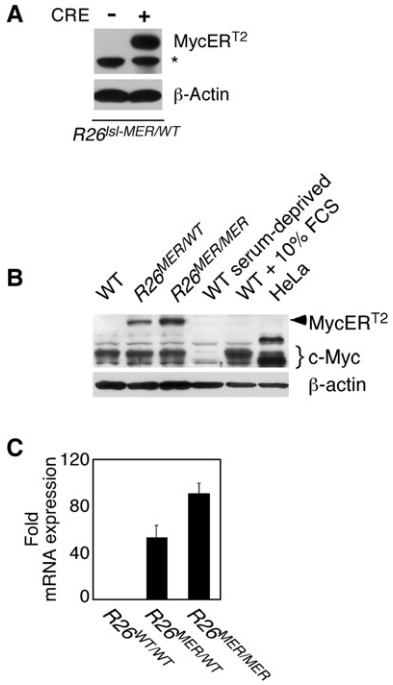

Figure 1. Characteristics of MycER^{T2} Expression in *R26$^{lsl-MER}$* Mouse Embryonic Fibroblasts

(A) *Rosa26*-driven MycER^{T2} expression in *R26$^{lsl-MER}$* mouse embryonic fibroblasts (MEFs) is Cre recombinase dependent and transgene dose dependent. *R26$^{lsl-MER/WT}$* MEFs were infected with retrovirus driving control vector (–) or Cre recombinase (+) and selected with puromycin for 3 days. Western blotting of whole-cell lysates with anti-human ERα antibody reveals expression of the predicted 92 kDa MycER^{T2} fusion protein. Asterisk denotes a nonspecific band.

(B) Simultaneous comparison of levels of endogenous Myc and MycER^{T2} in wild-type (WT), *R26$^{MER/WT}$*, and *R26$^{MER/MER}$* MEFs. MEFs were isolated from embryos of each genotype and cultured in complete growth medium/10% FBS. Equal numbers of cell equivalents from each lysate were western blotted with SC42 anti-Myc antibody, detecting an epitope common to endogenous Myc and MycER^{T2}. Extracts from serum-deprived WT MEFs and from WT MEFs 2 hr after addition of fresh medium were probed alongside, together with an equivalent number of HeLa cells, which overexpress c-Myc (~30,000 molecules per cell), for comparison (Moore et al., 1987).

(C) Dose-dependent expression of *MycER^{T2}* mRNA driven from the *Rosa26* locus. qPCR quantitation (mean + SEM) of *MycER^{T2}* mRNA isolated from WT, *R26$^{MER/WT}$*, and *R26$^{MER/MER}$* MEFs is shown normalized to *GUS* (n = 3).

likely a consequence of aberrantly sustained modulation of normal Myc target genes.

It is now generally accepted that spontaneous tumorigenesis is largely suppressed by the obligate coupling of proliferation to antioncogenic programs such as senescence and apoptosis (Evan and Littlewood, 1998; Lowe et al., 2004). Myc is a prototypical example of this phenomenon. Oncogenically activated Myc is a potent inducer of cell proliferation but also engages the ARF/p53 tumor suppressor pathway (Eischen et al., 1999; Kamijo et al., 1998; Schmitt et al., 1999; Zindy et al., 1998) and apoptosis (Askew et al., 1991; Evan et al., 1992), both tumor suppressor programs that antagonize cell expansion and restrict Myc's oncogenic potential. However, since Myc mediates the proliferation of normal cells, it is clear that activation of ARF/p53 and apoptosis must be restricted to situations wherein Myc is oncogenic. How cells distinguish between Myc that is activated by mitogenic signals and Myc that is oncogenically activated is unknown, although candidates include the abnormal persistence of oncogenic Myc, its activation outside the normal context of other mitogenic signals, and its overexpression.

To address these issues, we have developed a *Myc* transgenic mouse in which latent expression of the reversibly switchable variant of Myc, MycER^{T2}, is driven by the constitutive and ubiquitously active *Rosa26* promoter. Overt MycER^{T2} expression is then triggered in any target tissue by the hit-and-run action of Cre recombinase. Due to the relative weakness of the *Rosa26* promoter, the level of MycER expressed in tissues of such animals is very low and close to the physiological level of Myc following normal mitogen stimulation. We have used this model to define the oncogenic properties of Myc in vivo when deregulated but not significantly overexpressed. Our studies indicate that the level at which Myc is expressed plays an unforeseen and critical role in determining its oncogenic potential.

RESULTS

Generation of *R26-lsl-MER^{T2}* and *R26-MER^{T2}* Mice

The switchable, 4-hydroxytamoxifen (4-OHT)-dependent variant of Myc was generated by fusing Myc to the modified hormone-binding domain of the modified estrogen receptor ER^{T2} (Indra et al., 1999). To direct conditional expression of MycER^{T2} to target tissues, the cDNA was inserted downstream of the ubiquitously active *Rosa26* locus, preceded by a strong translational termination sequence flanked by *loxP* recombination sites. Murine embryonic stem cell clones transfected with the resulting targeting vector were screened by Southern blotting to identify single insertions into the *Rosa26* locus (see Figure S1 available online). Germline transmission of the *R26-lsl-MycER^{T2}* allele by chimeric mice was verified by PCR amplification across the Myc-ER^{T2} sequence junction. We refer to the resulting line of mice as *R26-lsl-MER^{T2}*.

To verify that MycER^{T2} expression is dependent upon excision of the translational termination element, we expressed Cre recombinase in *R26-lsl-MER^{T2}*-derived mouse embryonic fibroblasts (MEFs). Immunoblotting with anti-human ERα antibody demonstrated expression of the predicted 92 kDa MycER^{T2} fusion protein only in MEFs expressing Cre (Figure 1A). To directly compare in somatic cells and tissues the levels of *MycER^{T2}* expression driven from one or two copies of the *Rosa26* promoter with those of endogenous Myc, *R26-lsl-MER^{T2}* mice were crossed with the germline deletor strain *ZP3-Cre* (Lewandoski et al., 1997). *Rosa26*-driven MycER^{T2} is expressed in all somatic cells of such crosses, which we henceforth refer to as *R26^{MER}* mice. Relative levels of endogenous Myc and ectopic MycER^{T2} proteins in log-phase, serum-deprived, and serum-stimulated wild-type (WT) MEFs and in heterozygous *R26$^{MER/WT}$* and homozygous *R26$^{MER/MER}$* MEFs were then compared by immunoblotting cell extracts with SC42 anti-Myc antibody, which recognizes an epitope common to Myc and MycER^{T2}. MycER^{T2}, absent from WT MEFs, was expressed in homozygous *R26$^{MER/MER}$* cells at approximately twice the level present in heterozygous *R26$^{MER/WT}$* cells (Figure 1B). This was confirmed at the mRNA level by real-time quantitative PCR (qPCR) (Figure 1C). The steady-state level of MycER^{T2} in

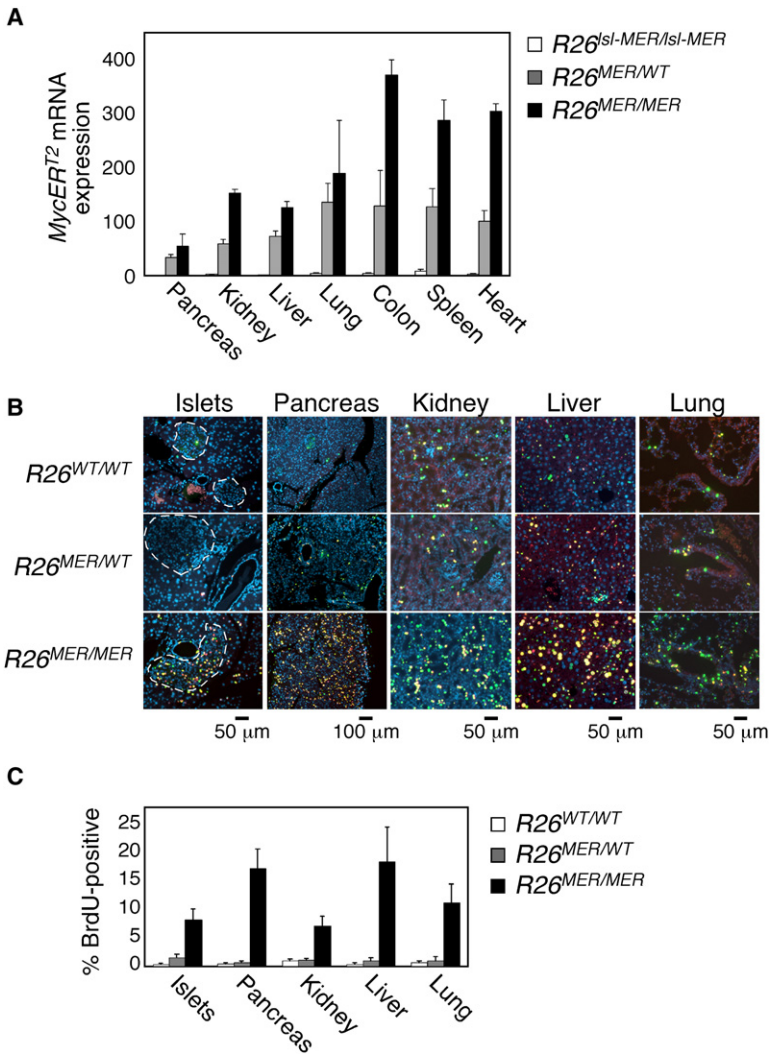

Figure 2. Dose-Dependent Induction of Proliferation by *Rosa26*-Driven MycER^{T2} In Vivo

(A) qPCR analysis of *MycER*^{T2} mRNA levels (mean + SEM) in selected organs from untreated adult *R26*$^{lsl\text{-}MER/lsl\text{-}MER}$ (white bars), *R26*$^{MER/WT}$ (gray bars), and *R26*$^{MER/MER}$ (black bars) mice, normalized to *GUS* (n = 3).

(B) Representative images of two-color immunofluorescent detection of BrdU/IdU incorporation, indicating instances of S phase progression in mice treated daily with tamoxifen for 6 days. Yellow-orange indicates BrdU incorporation (S phase on day 3); green indicates IdU incorporation (S phase on day 6).

(C) Quantification (mean + SEM) of BrdU incorporation in tissues of control, *R26*$^{MER/WT}$, and *R26*$^{MER/MER}$ mice at day 6.

R26$^{MER/WT}$ MEFs was a little lower than, and the MycER^{T2} levels in *R26*$^{MER/MER}$ MEFs a little higher than, that of endogenous Myc in logarithmically growing WT MEFs, and far below the ~30,000 Myc molecules per cell present in HeLa cells (Moore et al., 1987). MycER^{T2} protein half-life was short (15–20 min) (Figure S2A), essentially identical to that of endogenous Myc (Flinn et al., 1998; Ramsay et al., 1984). Unlike endogenous Myc, however, *R26*-driven MycER^{T2} expression was unaffected by serum status (Figure S2B). Above ~10,000 total Myc molecules per cell, Myc autoregulates, suppressing expression from its endogenous promoter (Penn et al., 1990). To ascertain whether MycER^{T2}, when activated, is expressed at a level sufficient to suppress endogenous Myc, we repeated the analysis in Figure 1B using MEFs treated continuously with 4-OHT to activate MycER^{T2}. We observed negligible downregulation of endogenous Myc upon activation of MycER^{T2} in either *R26*$^{MER/WT}$ or *R26*$^{MER/MER}$ MEFs (Figure S2C), consistent with the very low levels of MycER^{T2} present in *R26*^{MER} MEFs.

We used qPCR with selective primers both to quantitate the relative levels of endogenous *myc* versus *MycER*^{T2} mRNA in tissues of tamoxifen-treated and untreated *R26*$^{MER/MER}$ mice and to assess whether endogenous Myc expression is suppressed by *R26*-driven MycER^{T2} in vivo. As expected, levels of endogenous Myc were extremely low in nonproliferating tissues. In spleen, where cell proliferation is substantial, *MycER*^{T2} mRNA levels were comparable to those of endogenous *myc*. We observed no significant suppression of endogenous Myc upon activation of MycER^{T2} in any tissue aside from colonic epithelium (Figure S3).

Deregulated Expression of Low-Level Myc Induces Ectopic Proliferation in Multiple Adult Tissues

The relative contributions to oncogenesis made by Myc deregulation versus Myc overexpression remain unclear. The low level of deregulated MycER^{T2} expression in *R26*^{MER} tissues therefore provided a unique opportunity to ascertain the impact of Myc deregulation, without overt overexpression, in adult mouse tissues. To confirm *MycER*^{T2} expression in tissues, RNA was extracted from multiple organs from adult (2-month-old) homozygous *R26-lsl-MER*^{T2}, heterozygous *R26*$^{MER/WT}$, and homozygous *R26*$^{MER/MER}$ mice, and *MycER*^{T2} transcript levels were quantified by qPCR. *MycER*^{T2} mRNA was essentially undetectable in any organs of *R26-lsl-MER*^{T2} mice but exhibited gene-dose-dependent expression in all tested organs of *R26*^{MER} animals (Figure 2A).

To acutely activate MycER^{T2} in all tissues, tamoxifen was systemically administered daily for 6 days to adult *R26*$^{WT/WT}$, *R26*$^{MER/WT}$, and *R26*$^{MER/MER}$ mice. Proliferation in tissues was assessed by systemic administration of bromodeoxyuridine (BrdU) at day 3 followed by iododeoxyuridine (IdU) at day 6 to capture initial and delayed S phases (Burns and Kuan, 2005). BrdU and IdU incorporation in most tissues of tamoxifen-treated *R26*$^{MER/WT}$ animals (with the exception of colonic epithelium; see below) was indistinguishable from that in *R26*$^{WT/WT}$; by contrast, we saw a marked increase in incorporation of both BrdU and IdU in multiple tissues of homozygous *R26*$^{MER/MER}$ animals (Figure 2B), including exocrine pancreas, endocrine pancreas, kidney, liver, and lung. Of note, no proliferation was observed in skeletal or cardiac muscle, or in brain aside from the epithelial choroid plexus (Table S1). These data demonstrate that

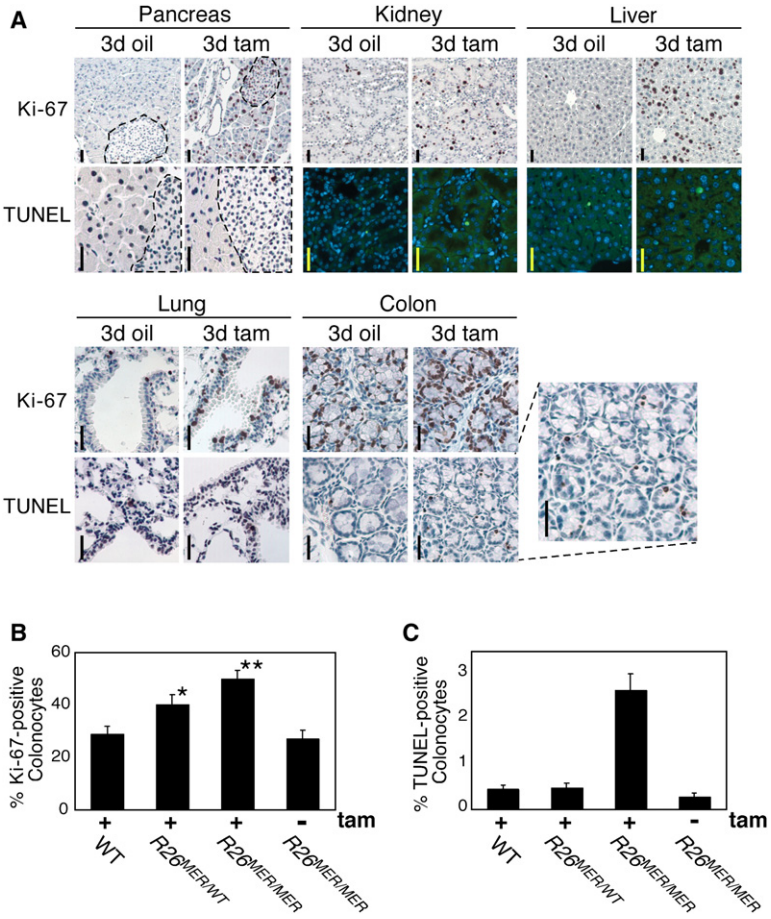

Figure 3. Widespread Myc-Induced Ectopic Proliferation Occurs without Apoptosis in *R26*$^{MER/MER}$ Mice

(A) Organs from adult *R26*$^{MER/MER}$ mice treated for 3 days with tamoxifen (tam) (n = 7) or oil carrier (n = 6), assessed for proliferation (Ki-67 staining) and apoptosis (TUNEL assay). Activation of MycER^{T2} drives abundant ectopic cell-cycle entry in multiple tissues (exocrine and endocrine pancreas, kidney, liver, lung, and colon are presented). However, with the exception of colon (inset), no tissues exhibited concomitant Myc-induced apoptosis. Scale bars = 25 μm.

(B) Quantification (mean + SEM) of Ki-67 staining in colon sections from tamoxifen-treated *R26*$^{WT/WT}$ (n = 4), *R26*$^{MER/WT}$ (n = 6), and *R26*$^{MER/MER}$ mice (n = 3) and from *R26*$^{MER/MER}$ mice treated with carrier (n = 3). t test analysis indicates that the increase in proliferation from *R26*$^{WT/WT}$ to *R26*$^{MER/WT}$ is significant (*p = 0.001), as is the increase from *R26*$^{MER/WT}$ to *R26*$^{MER/MER}$ (**p = 0.004).

(C) Quantification (mean + SEM) of TUNEL-positive cells in sections of colonic epithelium from the mice in (B).

deregulation of low-level Myc is alone sufficient to drive sustained proliferation in a significant subset of tissues. However, MycER^{T2}-induced proliferation was only evident in homozygous *R26*$^{MER/MER}$ tissues (Figure 2C), indicating that a critical minimum threshold level of Myc is needed to drive proliferation in "permissive" tissues and that this threshold is straddled by the levels of MycER^{T2} expression in hetero- and homozygous *Rosa26-MER*^{T2} mice. Ipso facto, we conclude that the ectopic Myc activity in tissues of homozygous *R26*$^{MER/MER}$ mice is close to the minimum required to drive ectopic proliferation.

Different Threshold Levels of Myc Trigger Myc-Induced Proliferation versus Induction of Apoptosis and *ARF*

Myc-induced apoptosis is a key intrinsic tumor suppressor mechanism that limits Myc's oncogenic potential. However, the factors that determine whether proliferation or cell death is the predominant outcome of Myc activation remain unclear. To ascertain whether activation of low-level MycER^{T2} induces apoptosis in tissues in vivo, Myc was activated systemically in adult *R26*$^{MER/MER}$ mice for 0, 3, or 6 days, and tissue sections from multiple organs were then probed with Ki-67-specific antibody to identify cells in cycle and by TUNEL to identify apoptotic cells. As with our BrdU/IdU incorporation data, proliferation was robustly induced by 3 days of MycER^{T2} activation in the same proliferation-permissive organs as above, remaining elevated at 6 days in pancreatic islets, kidney, and lung (Figure 3A and Figure S4; summarized in Table S1). However, we observed no Myc-induced apoptosis in any tissues (again, with the exception of colonic epithelium; see below). We conclude that quasiphysiological levels of deregulated Myc are sufficient to drive proliferation in most permissive tissues without engaging concomitant apoptosis.

As mentioned, colonic epithelium of *R26*$^{MER/MER}$ mice was a notable exception to the above pattern: here, Myc activation induced abundant apoptosis. Provocatively, out of all *R26*^{MER} tissues tested, colonic epithelium exhibited the highest level of MycER^{T2} expression (Figure 2A). Indeed, even the single allele of *MycER*^{T2} in heterozygous *R26*$^{MER/WT}$ mice drove Myc expression sufficient to trigger proliferation in colonic epithelium upon activation (p = 0.001; Figure 3B). In colonic epithelium of homozygous *R26*$^{MER/MER}$ animals (Figure 3B), Myc-induced proliferation was even more marked, although accompanied by apoptosis (Figure 3C). Together, these observations intimated that induction of apoptosis in vivo might require a higher level of Myc than proliferation.

Like apoptosis, induction of p19^{ARF} by oncogenic Myc is a critical restraint to Myc oncogenesis that, by activating p53 through inhibition of Mdm2 (Kamijo et al., 1998; Weber et al., 1999; Zindy et al., 1998), can both drive apoptosis (Hermeking and Eick, 1994; Wagner et al., 1994; Zindy et al., 1998) and suppress proliferation (Finch et al., 2006). p19^{ARF} may also exert p53-independent tumor-suppressive functions (Lowe and Sherr, 2003), in part mediated by direct binding and functional inactivation of Myc (Datta et al., 2004; Qi et al., 2004). To ascertain whether the low yet mitogenic level of deregulated Myc in tissues of *R26*$^{MER/MER}$ mice is sufficient to induce *ARF* expression, we quantified *p19*^{ARF} mRNA and protein expression following MycER^{T2} activation (Figure 4A). Notwithstanding some variability in measured basal levels of *ARF* mRNA between tissues and individual isolates, we saw no measurable induction by Myc of *ARF* mRNA or protein in any tissue except, once again, colonic epithelium. Because it has recently been suggested that even extremely low levels of p19^{ARF} may exert tumor-suppressive

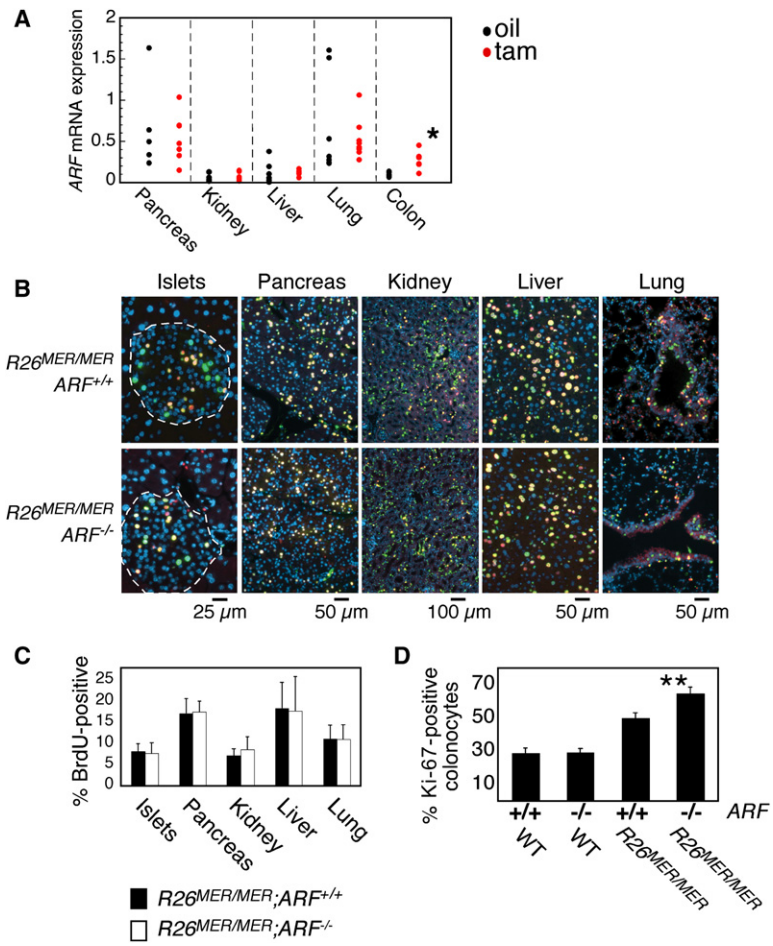

Figure 4. Activation of MycER^{T2} in Most Tissues of *R26$^{MER/MER}$* Mice Does Not Induce the p19^{ARF} Tumor Suppressor

(A) qPCR analysis for expression of *ARF* mRNA in organs from adult *R26$^{MER/MER}$* mice treated for 3 days with tamoxifen (n = 7) or oil carrier (n = 7), normalized to *GUS*. No *ARF* was induced by MycER^{T2} activation in any tissue tested, except for colonic epithelium, where it was statistically significant (*p = 0.004).

(B) Representative two-color immunofluorescence images of tissues from *R26$^{MER/MER}$;ARF$^{+/+}$* (n = 7) and *R26$^{MER/MER}$;ARF$^{-/-}$* (n = 4) mice injected daily with tamoxifen for 6 days. Mice were systemically pulsed with BrdU on day 2 and IdU on day 6, as in Figure 2, to identify cells in S phase on day 2 (yellow-orange) and day 6 (green).

(C) Quantification (mean + SEM) of BrdU incorporation on day 6. Note that the *ARF$^{+/+}$* data are the same as those presented in Figure 2C.

(D) Quantification (mean + SEM) of Ki-67 staining of colon sections from the indicated mice treated for 3 days with tamoxifen. Data for *ARF$^{+/+}$* samples are the same as those presented in Figure 3B. *R26$^{WT/WT}$;ARF$^{-/-}$* (n = 3); *R26$^{MER/MER}$;ARF$^{-/-}$* (n = 2).

activity (Bertwistle and Sherr, 2007), we also confirmed genetically that the Myc phenotypes we observed in vivo were p19^{ARF} independent by crossing the *R26$^{MER/MER}$* mice into the *ARF$^{-/-}$* background. *ARF* status had no impact on the extent, kinetics, or duration of Myc-induced proliferation in most *R26$^{MER/MER}$* mouse tissues (Figures 4B and 4C). Together, these data show that the low level of deregulated Myc expressed in most proliferation-permissive tissues of *R26$^{MER/MER}$* mice, while adequate to induce widespread proliferation, is insufficient to engage the p19^{ARF}/p53 tumor suppressor pathway.

R26$^{MER/MER}$ colonic epithelium was, again, an exception to the above: Myc activation induced a >2-fold induction of *ARF* mRNA (Figure 4A; p = 0.004) in colon, and induction of p19^{ARF} was confirmed by immunoblotting of colonocyte lysates prepared from fresh tissue (data not shown). Furthermore, Myc-induced colonocyte proliferation was significantly enhanced in the *ARF$^{-/-}$* background (Figure 4D). As with apoptosis, this is consistent with the notion that induction of p19^{ARF} requires higher levels of Myc than proliferation.

To ascertain directly whether the thresholds for Myc-induced proliferation versus tumor suppression (induction of apoptosis and *ARF*) are set at different levels of Myc expression in vivo, we used the *pIns-MycER^{TAM}* β cell mouse model, in which the powerful rat insulin promoter drives high-level expression of 4-OHT-dependent MycER in pancreatic β cells (Figure S5A). We previously showed that activation of Myc in this model efficiently triggers β cell proliferation but that this is rapidly curtailed by concomitant activation of both apoptosis and induction of nucleolar p19^{ARF} (Figures S5A, S5B, and S6) (Finch et al., 2006; Pelengaris et al., 2002). qPCR and immunoblot analyses of pancreatic islets isolated from *pIns-MycER^{TAM}*, *R26$^{MER/WT}$*, and *R26$^{MER/MER}$* mice indicated that *MycER^{TAM}* mRNA and protein expression were ~15-fold higher in *pIns-MycER^{TAM}* islets than that of *MycER^{T2}* in islets from homozygous *R26$^{MER/MER}$* animals (Figure 5A; Figure S5C). To directly compare the net outcome of acute Myc activation in *pIns-MycER^{TAM}* versus *Rosa26$^{MER/MER}$* islets, we activated MycER in vivo for 3 and 6 days and then stained pancreatic tissue sections for markers of proliferation (Ki-67) and apoptosis (TUNEL). As expected (Finch et al., 2006; Pelengaris et al., 2002), high levels of activated Myc in the *pIns-MycER^{TAM}* islets induced proliferation together with both *ARF* induction and overwhelming β cell apoptosis, resulting in rapid islet involution. By contrast, activation of low-level Myc in islets of *R26$^{MER/MER}$* mice drove proliferation without any attendant apoptosis or islet involution, resulting in progressive islet hyperplasia (Figure 5B; Figure S7). Likewise, activation of low-level MycER^{T2} in lung epithelium of *R26$^{MER/MER}$* mice failed to elicit *ARF* expression, whereas the high levels of MycER^{T2} delivered into lung epithelium by adenoviral vector potently induced *ARF* upon tamoxifen activation (Figure S5D). Hence, in both β cells and lung in vivo, deregulated Myc is competent to activate intrinsic tumor suppression pathways so long as it is expressed at elevated levels.

There are two plausible explanations for how different threshold levels of Myc might preferentially trigger proliferation versus apoptosis. It could be that low and high levels of Myc engage different sets of target genes, perhaps due to differing affinity Myc-binding promoter/enhancer elements (i.e., Myc discriminates)

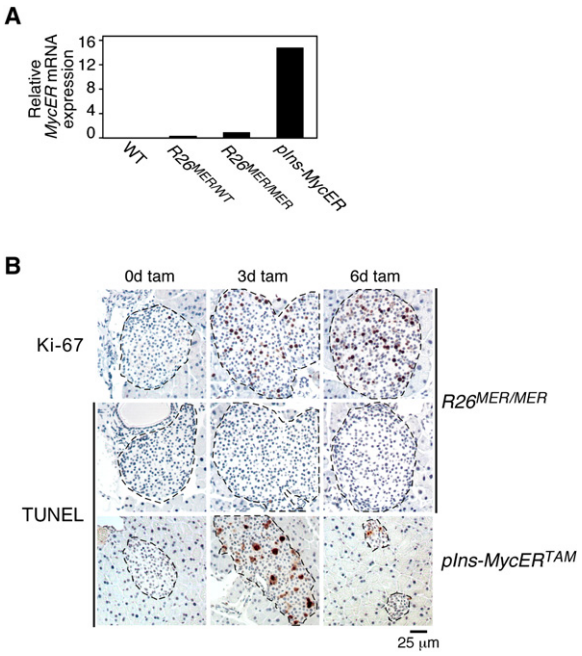

Figure 5. Induction of Apoptosis Requires Higher Levels of Deregulated Myc than Induction of Ectopic Proliferation

(A) qPCR analysis of *MycER* mRNA expression in islets isolated from disaggregated pancreata of untreated designated mice, pooled according to genotype ($n > 2$ per cohort). Expression was normalized to *GUS*, and results are expressed relative to $MycER^{T2}$ mRNA in $R26^{MER/MER}$ islets.

(B) TUNEL staining of pancreatic islets from $R26^{MER/MER}$ mice treated with tamoxifen for 3 ($n = 7$) or 6 ($n = 6$) days, with matched samples from similarly treated $pIns\text{-}MycER^{TAM}$ mice (lower panels). Ki-67 staining of adjacent sections from $R26^{MER/MER}$ pancreata (upper panels) demonstrates tamoxifen-induced functionality of *Rosa26*-driven $MycER^{T2}$ protein.

(Figure S8A). In this model, low-level Myc simply fails to activate the apoptotic transcriptional program. Alternatively, Myc might regulate the same genes in each case, but to a greater extent when expressed at a higher level, and the differential Myc outputs arise from different thresholds at which the proliferative and apoptotic programs fire (i.e., downstream factors decide) (Figure S8B). In this case, low-level Myc still activates the apoptotic program, but to a level insufficient to trigger it. We reasoned that if the second model holds, subapoptotic low-level Myc should, by priming the apoptotic machinery, sensitize cells to induction of apoptosis by other triggers. We therefore exposed $R26^{MER/MER}$ mice to both tamoxifen, to activate $MycER^{T2}$ in tissues, and a subapoptotic dose of the cytotoxic agent doxorubicin. The combination of both subapoptotic stimuli triggered significant apoptosis in several tissues, including pancreatic islets and liver, and significantly exacerbated the extent of Myc-induced apoptosis in colonic epithelium (Figures 6A and 6B). Thus, low-level deregulated Myc, although insufficient to trigger apoptosis itself, nonetheless engages the Myc apoptotic program.

Deregulation of Low-Level Myc Is Tumorigenic

Although low-level deregulated Myc is sufficient to drive ectopic proliferation in tissues, it remained possible that actual tumorigenicity, like apoptosis and *ARF* induction, requires higher-level Myc expression. To investigate this, we used intranasal delivery of recombinant adenovirus-expressing Cre (Ad-Cre) to trigger sporadic expression of $MycER^{T2}$ in lung epithelia of homozygous $R26^{lsl\text{-}MER/lsl\text{-}MER}$ mice. $MycER^{T2}$ was then activated by daily systemic administration of tamoxifen for 3 ($n = 4$) or 6 ($n = 5$) weeks. After 3 weeks of sustained Myc activity, bronchiolar (Figure 7A, panel 1) and bronchioalveolar junction regions (panel 2) of $R26^{lsl\text{-}MER/lsl\text{-}MER}$ lungs exhibited multiple hyperplastic and dysplastic epithelial foci with pseudostratification and occasional micropapillary tuft formation. After 6 weeks, more extensive micropapillary and papillary hyperplasia was clearly evident (panel 3), with several bronchioles exhibiting Clara cell hyperplasia and sloughing into the airway lumen (panel 4). These Myc-induced lesions closely resemble the early bronchioalveolar lesions that develop 6–8 weeks after sporadic activation of oncogenic $K\text{-}Ras^{G12D}$ driven from the endogenous *KRas2* promoter (Jackson et al., 2001, 2005; Johnson et al., 2001).

Individually, Myc or Ras is usually insufficient to drive full tumor progression, but together they exhibit potent oncogenic cooperation (Land et al., 1983). To ascertain whether low-level deregulated Myc cooperates with Ras oncogenesis in lung epithelium in vivo, we crossed homozygous $R26^{lsl\text{-}MER/lsl\text{-}MER}$ and heterozygous $R26^{lsl\text{-}MER/WT}$ mice into the conditional $LSL\text{-}K\text{-}Ras^{G12D}$ model (Jackson et al., 2001, 2005; Johnson et al., 2001). Sporadic coexpression of both oncogenes in lung epithelium was triggered by Ad-Cre inhalation, and $MycER^{T2}$ was then activated by tamoxifen administration. Induction of $K\text{-}Ras^{G12D}$ alone elicited atypical adenomatous hyperplasias within 2 weeks, small adenomas by 6 weeks postinfection, and overt adenocarcinomas only after 16–26 weeks (Jackson et al., 2001, 2005). Identical hyperplastic and dysplastic bronchiolar lesions arose with identical kinetics and efficiency in $LSL\text{-}K\text{-}Ras^{G12D};R26^{lsl\text{-}MER/lsl\text{-}MER}$ mice that were not given tamoxifen (i.e., only Ras was activated) (Figure 7B, panels 1–4) and in control $LSL\text{-}K\text{-}Ras^{G12D}$-only mice treated with either oil ($n = 2$) or tamoxifen ($n = 8$; data not shown). By contrast, activation of $MycER^{T2}$ together with $K\text{-}Ras^{G12D}$ profoundly accelerated tumor progression compared to $K\text{-}Ras^{G12D}$ alone in homozygous, but not heterozygous, $Rosa26\text{-}lsl\text{-}MER^{T2}$ animals. By 6 weeks post Ad-Cre infection, papillary adenomas were both more numerous and significantly larger (panels 5 and 6) in coactivated mice, some having already progressed to invasive adenocarcinoma (panels 9–12). Such adenocarcinomas were poorly differentiated, growing as small tumor clusters with individual tumor cells embedded within desmoplastic stroma (panel 10). Whereas few mitotic figures were evident in the lesions induced by $K\text{-}Ras^{G12D}$ alone, they were readily detectable in the bronchiolar lesions (compare panel 4 and panel 8), adenomas (panel 11), and adenocarcinomas (panels 11 and 12) induced by $K\text{-}Ras^{G12D}$ and $MycER^{T2}$ together, indicating that low-level expression of deregulated Myc confers a significantly higher level of tumor cell proliferation and is possessed of potent tumorigenic activity.

DISCUSSION

Uncontrolled proliferation of somatic cells is an ever-present risk for large, long-lived organisms like vertebrates whose tissues harbor cells that proliferate throughout life. Hence, multiple surveillance mechanisms have evolved to suppress the emergence

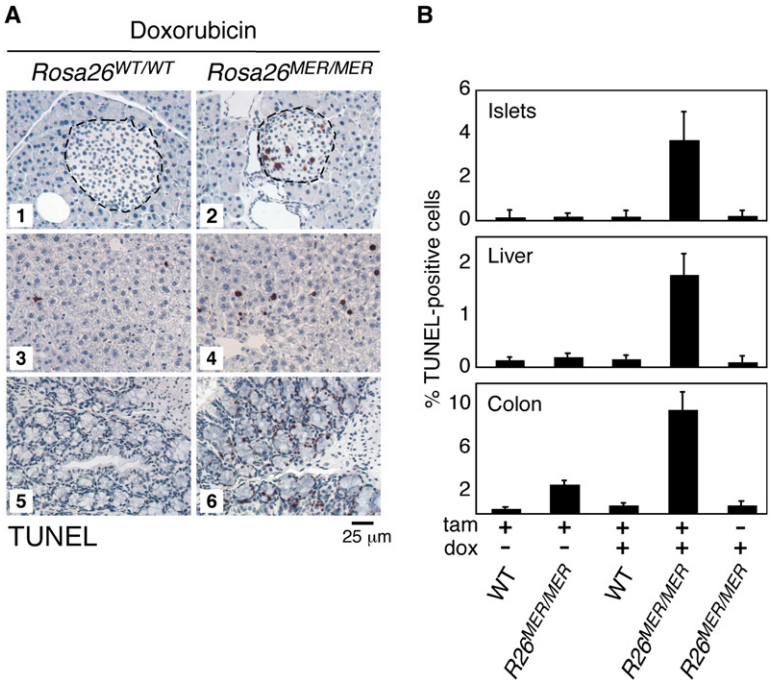

Figure 6. Subapoptotic Myc Synergizes with Subapoptotic Doxorubicin to Induce Apoptosis in Multiple Tissues

(A) TUNEL staining of pancreatic islets (panels 1 and 2), liver (panels 3 and 4), and colon (panels 5 and 6) from $R26^{WT/WT}$ (n = 2) and $R26^{MER/MER}$ (n = 4) mice treated for 3 days with tamoxifen and overnight with 10 mg/kg doxorubicin.

(B) Quantification (mean + SEM) of TUNEL staining in sections from pancreas (islets), liver, and colon from the mice in (A) treated with tamoxifen and/or doxorubicin. (n = 2–4 mice per cohort).

and propagation of tumor cells. One of these involves the tight coupling of tumor suppression to the programs that drive cell proliferation, a phenomenon dubbed "intrinsic tumor suppression" (Lowe et al., 2004). Such obligate coupling serves to annul the immediate growth advantage afforded by oncogenic activation of the cell's proliferative machinery. The Myc transcription factor is a prototypical example of this. In normal cells, Myc coordinates and drives the diverse intra- and extracellular programs required for orderly expansion of normal somatic cells. However, oncogenic Myc triggers the ARF/p53 tumor suppressor pathway and apoptosis, two potent tumor suppressor programs that efficiently restrain Myc's oncogenic potential (Evan and Littlewood, 1998; Lowe et al., 2004). However, for intrinsic tumor suppression to be compatible with the orderly proliferation in normal tissues, cells must accurately and reliably discriminate between normal mitogenic and oncogenic signaling; how they do this is unclear. One potential distinctive hallmark of oncogenic signals is their aberrant context: in normal cells, Myc is never activated alone but always in the context of collateral signaling pathways. Another possibility is the unusual persistence of oncogenic Myc—endogenous Myc activity is tightly mitogen dependent and episodic. Finally, as a consequence of its mutation or its relentless induction by other oncogenes, Myc is usually present at significantly higher levels in tumors than in normal cells.

The undeniable importance of intrinsic tumor suppression is demonstrated by the profound acceleration of oncogenesis in *Myc* transgenic mouse models afforded by genetic lesions that block apoptosis or circumvent the ARF/p53 pathway. Unfortunately, classical transgenic Myc models employ highly active tissue-specific promoter/enhancer elements to drive transgenic Myc expression in the requisite target tissue. Hence, Myc is both deregulated and elevated, making it impossible to ascertain which specific aberrant feature of oncogenic Myc engages tumor suppression. To circumvent this shortcoming, we made use of the relatively weak, but ubiquitous, *Rosa26* promoter to drive low-level deregulated expression of the switchable form of Myc, $MycER^{T2}$, in target tissues. A $MycER^{T2}$ open reading frame was inserted downstream of the endogenous *Rosa26* promoter, but its expression was blocked by an intervening transcriptional stop element flanked by *loxP* recombination sites. Hit-and-run excision of the stop element by Cre recombinase triggers targeted expression of $MycER^{T2}$; however, $MycER^{T2}$ activity is dependent upon continuous provision of 4-OHT ligand.

To ascertain the level at which the *Rosa26* promoter drives $MycER^{T2}$ expression in adult tissues, we crossed mice harboring one or two copies of *Rosa26-LSL-MycER^{T2}* into the *ZP3-Cre* background, which excises the floxed stop element in the egg. The resulting $R26^{MER}$ animals express $MycER^{T2}$ from the *Rosa26* promoter in all tissues. In all $R26^{MER}$ tissues tested, $MycER^{T2}$ expression levels were broadly comparable, although somewhat higher in colonic epithelium. In all tissues examined, homozygous $R26^{MER/MER}$ mice expressed approximately twice as much *MycER^{T2}* mRNA and protein as their heterozygous $R26^{MER/WT}$ littermates.

Acute activation of $MycER^{T2}$ in tissues of homozygous $R26^{MER/MER}$ mice triggered widespread ectopic proliferation in many tissues, including endocrine and exocrine pancreas, liver, kidney epithelium, lung, skin, and lymphoid organs. In most instances, proliferation was sustained to at least 6 days of continuous Myc activation: analysis beyond this time was curtailed by precipitous onset of anemia and dehydration that coincided with intestinal hemorrhage and necessitated euthanasia. In contrast to homozygous $R26^{MER/MER}$ mice, activation of $MycER^{T2}$ in heterozygous $R26^{MER/WT}$ animals elicited no increased proliferation in any tissues except colon and, weakly, spleen red pulp. Given that there is only a 2-fold difference in $MycER^{T2}$ levels in heterozygous versus homozygous $R26^{MER}$ mice, this defines a sharp minimum threshold level of intracellular Myc required to elicit ectopic proliferation in vivo. It also indicates that the level of ectopic activated $MycER^{T2}$ in homozygous $R26^{MER/MER}$ tissues is close to the minimum necessary to drive ectopic proliferation. It is interesting that the level of ectopic $MycER^{T2}$ in heterozygous $R26^{MER/WT}$ tissues, while comparable to that of endogenous Myc in MEFs proliferating in response to serum, is insufficient to drive those tissues into the cell cycle. We

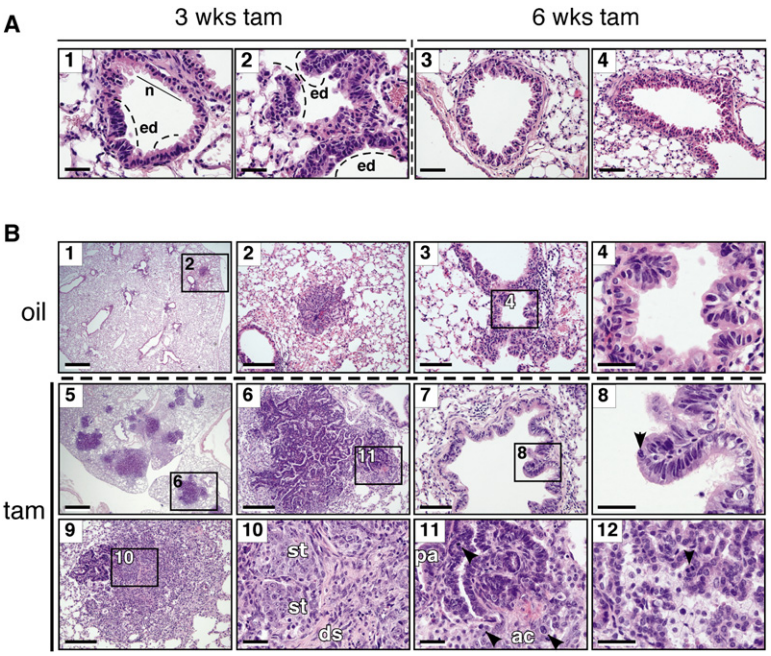

Figure 7. Low-Level Deregulated Myc Is Tumorigenic In Vivo

(A) Representative images of hematoxylin and eosin (H&E)-stained lungs from tamoxifen-treated, Ad-Cre-infected *R26*$^{lsl\text{-}MER/lsl\text{-}MER}$ mice showing multiple preneoplastic pulmonary lesions. Panels 1 and 2: localized epithelial dysplasia (ed) evident in airway epithelium (panel 1) and bronchioalveolar junctions (panel 2) after 3 weeks of sustained MycER^{T2} activation. Compare with normal bronchiolar epithelium (n). Scale bars = 20 μm. Panels 3 and 4: micropapillary and papillary Clara cell hyperplasia present after 6 weeks of sustained MycER^{T2} activation. Scale bars = 40 μm.

(B) H&E-stained lungs from Ad-Cre-infected *LSL-K-Ras*^{G12D}*;R26*$^{lsl\text{-}MER/lsl\text{-}MER}$ mice treated with oil carrier (n = 3, panels 1–4) or tamoxifen (n = 6, panels 5–12) for 6 weeks. Panels 1, 2, 5, and 6: size comparison between tumors driven by K-Ras^{G12D} alone (1 and 2) and K-Ras^{G12D}/MycER^{T2} combined (5 and 6). Scale bars = 0.4 μm in panels 1 and 5 and 100 μm in panels 2 and 6. The numbered rectangular regions within panels 1, 3, 5–7, and 9 are shown enlarged in panels 2, 4, 6, 11, 8, and 10, respectively. Panels 3, 4, 7, and 8: micropapillary bronchiolar hyperplasia and dysplasia driven by K-Ras^{G12D} alone (3 and 4) and K-Ras^{G12D}/MycER^{T2} combined (7 and 8). Arrowhead in panel 8 points to a mitotic figure. Scale bars = 50 μm in panels 3 and 7 and 20 μm in panels 4 and 8. Panels 9–12: progression to carcinoma observed after 6 weeks of combined Kras^{G12D}/MycER^{T2}-driven oncogenesis. Scale bars = 100 μm in panel 9 and 20 μm in panels 10–12. Panel 10: nests of solid tumor (st) and isolated tumor cells surrounded by desmoplastic stroma (ds). Panels 11 and 12: mitotic figures (arrowheads) present in combined K-Ras^{G12D}/MycER^{T2}-driven papillary adenoma (pa) and adenocarcinoma (ac).

presume that this reflects the fact that serum mitogens engage both Myc and multiple, additional synergistic signaling pathways. By contrast, Myc is the sole engine of proliferation in *R26*$^{MER/WT}$ cells. It is also possible that activated MycER^{T2} has reduced specific activity compared to wild-type Myc protein, leading to an overestimation of the level of functional Myc in *R26*^{MER} tissues. Of note, while MycER^{T2} was expressed in all *R26*$^{MER/MER}$ tissues tested, some failed to proliferate when MycER^{T2} was activated. Why this should be is unclear, but it is likely that some cell types are constitutionally unable to proliferate due to structural constraints or lack of critical components of the cell-cycle machinery. Other cell types may be competent to proliferate only in response to higher levels of Myc than are expressed in *R26*$^{MER/MER}$ tissues. An obvious example of this would be the many differentiated cell types that express appreciable levels of Mad proteins (Chin et al., 1995; Queva et al., 1998; Vastrik et al., 1995), which mitigate Myc action by competing with Myc for Max.

Not only is low-level constitutive expression of MycER^{T2} sufficient to induce and maintain aberrant proliferation in many normal *R26*$^{MER/MER}$ tissues in vivo, it is also oncogenic, efficiently driving early-stage tumorigenesis in lung epithelium and, in cooperation with activated Ras, full progression to invasive adenocarcinoma (Figure 7). Nonetheless, even though *Rosa26*-driven Myc is oncogenic and both deregulated and active out of normal mitogenic context, it fails to induce either apoptosis or measurable *ARF* expression in most tissue types. This indicates a fundamental difference in how Myc engages its oncogenic and tumor-suppressive outputs. The one notable exception to this is colonic epithelium, and since this is the *R26*^{MER} tissue with the highest level of MycER^{T2} expression, we hypothesized that overexpression of Myc is likely the determining trigger of intrinsic tumor suppression. We confirmed this directly in pancreatic β cells and lung epithelium: in both tissues, further elevation of Myc levels triggered both apoptosis and *ARF*. Therefore, we conclude that it is the aberrant intensity of oncogenic Myc, and not its abnormal persistence or context, that triggers intrinsic tumor suppression. Recently, it was shown that induction of both *ARF* and replicative senescence by activated Ras in vivo also requires overexpression of the activated oncoprotein (Sarkisian et al., 2007). Hence, preternaturally high intensity appears to be the general metric by which cells discriminate between normal and oncogenic signals. However, we do not discount the possibility that even low levels of deregulated Myc may be sufficient in some cell lineages to engage apoptosis and/or ARF expression at some level that suppresses tumor initiation. Indeed, data from studies on transgenic Myc in the well-characterized *Eμ-myc* lymphoma model suggest that even very low Myc levels can, at some point in tumor evolution, contribute to the selective pressure to inactivate ARF or p53 (Bertwistle and Sherr, 2007).

Paradoxically, our data suggest that low-level deregulated Myc may be a more efficient initiator of oncogenesis than Myc that is overexpressed, since the latter can be tolerated only by cells that have already lost their tumor suppressor pathways. Indeed, high initial levels of Myc may even impede onset of tumorigenesis, a conclusion consistent with surprising recent findings that coexpression of Myc delays the mean latency of tumor onset in a transgenic *RasG12D* lung tumor model (Tran et al., 2008). This elegant study used the *CC10* promoter to drive doxycycline-dependent Myc expression in Clara cells and alveolar type II pneumocytes at very high levels, at least ten times the quasiphysiological level of MycER^{T2} in lung epithelium of *R26*$^{MER/MER}$ mice (Figure 2A). As our data show, such high levels of Myc breach the *ARF*/apoptotic triggering threshold, and by engaging

intrinsic tumor suppression, this has the immediate effect of staunching tumorigenesis. By contrast, oncogenic cooperation in the *LSL-K-Ras^{G12D};R26$^{lsl\text{-}MER/lsl\text{-}MER}$* mouse is efficient because it involves levels of oncogenic Myc (and presumably Ras) that are too low to trigger significant intrinsic tumor suppression. We surmise that low-level oncogene expression may be a general characteristic of early-stage spontaneous tumors and that most tumors evolve via a two-stage selective process. Early on, when tumor suppressor pathways remain intact, selection strongly favors low-level oncogene activity and the relatively indolent clonal expansion it confers. Elevated oncogene activity, together with the increased aggressiveness it confers on tumors, becomes subject to positive selection only once the appropriate intrinsic tumor suppressor pathways have been eroded by sporadic mutation.

How might different levels of Myc trigger such distinct biological outputs? One possibility is that Myc-induced ARF/p53 and apoptosis are mediated by a distinct set of target genes, perhaps those with lower-affinity promoter/enhancer elements that respond only to elevated Myc levels (Figure S5A). Alternatively, Myc might regulate identical sets of gene targets in both cases, although to lesser or greater overall extents when Myc is low or high, respectively, with net outcome determined by the different execution thresholds of each output program (Figure S5B). To distinguish between the two possibilities, we asked whether expression of Myc at levels that trigger no overt apoptosis nonetheless reduces the threshold for induction of apoptosis by other insults. MycER^{T2} was globally activated in *R26$^{MER/MER}$* mice, which were then systemically exposed to the cytotoxic drug doxorubicin at a dose that was itself subapoptotic. The combination of sublethal Myc and doxorubicin induced apoptosis in several tissues. Myc-induced apoptosis is mediated through the intrinsic mitochondrial pathway (Juin et al., 1999) that is triggered when the antiapoptotic buffering of the Bcl-2/Bcl-x$_L$ proteins is neutralized by the sum of activated BH3 proteins. Our data imply that low-level Myc still activates its requisite BH3 apoptotic effectors, but to a level insufficient to neutralize Bcl-2/Bcl-x$_L$ without the cooperation of collateral apoptotic signals. Of note, we saw no correlation between Myc-induced proliferation and Myc-induced sensitivity to doxorubicin in different tissues, indicating that Myc-dependent doxorubicin sensitivity is not merely a consequence of these tissues' increased proliferative status but reflects an inherent variability in the innate sensitivity to Myc-induced apoptosis among different cell types in vivo. Indeed, even in any one cell type, the threshold for triggering Myc-induced apoptosis is highly dependent upon changes in relative levels of the Bcl-2-family proteins (Bissonnette et al., 1992; Fanidi et al., 1992; Juin et al., 2002; Wagner et al., 1993) and availability of survival signals (Harrington et al., 1994a, 1994b). Hence, the level of Myc required to trigger apoptosis is not an innate, fixed property of a cell but is exquisitely dependent upon the cell's internal state and microenvironment. Importantly, such tissue-specific variations in the threshold set points for Myc oncogenic and apoptotic output mean that the innate susceptibilities of different tissues to Myc-driven oncogenesis will depend greatly on the level at which oncogenic Myc is expressed. Whether the operational threshold at which Myc triggers ARF is similarly subject to such protean, cell-type-specific influences is unknown. One final implication of the different firing thresholds at which Myc's distinct outputs (proliferation and tumor suppression) are set is that relatively subtle changes in overall Myc activity may suffice to shift above or below each specific threshold, thereby triggering dramatically different outcomes. Likewise, it is possible that mutations that merely augment or degrade overall Myc activity, by shifting the effective level of Myc above or below different output thresholds, could appear selective for specific Myc functions.

EXPERIMENTAL PROCEDURES

Generation of *Rosa26-MER* Targeting Vector and Mice

c-*myc* cDNA lacking a stop codon was excised from *pBabe-MycER^{TAM}* (Littlewood et al., 1995) and annealed to T2 point-mutated ligand-binding domain of human estrogen receptor from *pCreER^{T2}* (Indra et al., 1999), followed by the *IRES-EGFP* fragment (generously provided by D. Dankort and M. McMahon, UCSF), generating *c-MycER^{T2}-IRES-EGFP* (*MIE*). This *MIE* fragment was then incorporated into the previously described *Rosa26* vector *pBigT* (Srinivas et al., 2001) and excised, incorporating both the floxed stop/*neomycin^R* cassette and *MIE*. The final vector, *pRosa26fsMIE*, was linearized with SwaI and transfected into murine embryonic stem cells, and neomycin-resistant clones were identified by Southern blotting. An internal probe was generated by random priming from a gel-purified 1.6 kb NcoI/HindIII fragment of *pR26-PAS*, further digested with AscI to separate it from comigrating DNA. An external probe was generated by random priming from a 330 bp NotI fragment of the *Rosa26* promoter, generously provided by P. Soriano (Fred Hutchinson Cancer Research Center, Seattle). Chimeric mice were initially bred with C57BL/6 mice until germline transmission of the allele was observed. The consequent *R26-lsl-MycER^{T2}* mouse line was bred to C57BL/6, then alternately to FVBN, and maintained on a mixed FVBN/C57BL/6 background.

Other Mouse Strains, Procedures, and Genotyping

All procedures involving mice were performed in accordance with protocol number AN 076148 (UCSF Institutional Animal Care and Use Committee). *Zp3-Cre* (Lewandoski et al., 1997), *LSL-K-Ras^{G12D}* (Jackson et al., 2001), *p19$^{ARF-/-}$* (Kamijo et al., 1999), and *pIns-MycER^{TAM}* (Pelengaris et al., 2002) mice have been described previously. Tamoxifen (Sigma), dissolved in peanut oil, was administered daily by intraperitoneal (i.p.) injection for a maximum of 6 weeks at a dose of 1 mg/20 g body mass per day. For BrdU/IdU double labeling, bromodeoxyuridine (Sigma) and iododeoxyuridine (Sigma) dissolved in Tris-buffered saline were injected i.p. three times at 6 hr intervals on day 3, while IdU was injected one time 5–6 hr prior to harvest 1 day after the last tamoxifen injection (day 6). To deliver adenovirus-Cre recombinase (Ad-Cre), mice were anesthetized with 2.5% Avertin (250 μl/20 g body mass) and 5 × 10^7 plaque-forming units of Ad-Cre were administered as described previously (Fasbender et al., 1998). Details of primer/probe sets used for genotyping and expression analysis can be found in the Supplemental Data.

Cell Culture and Immunoblotting

Embryonic fibroblasts were isolated from E13.5 *R26-lsl-MycER^{T2}* and *R26-MycER^{T2}* mice. Whole-cell lysates were prepared by dissolving cells in Tween lysis buffer (150 mM NaCl, 50 mM HEPES [pH 7.5], 1 mM EDTA, 2.5 mM EGTA, 0.1% Tween 20 plus Complete protease inhibitor cocktail [PIs; Roche]) followed by sonication. Nuclear extracts were prepared in low-salt buffer (20 mM KCl, 10 mM HEPES [pH 7.5], 1 mM $MgCl_2$, 1 mM $CaCl_2$, 0.1% Triton X-100 plus PIs). For liver extracts, freshly isolated livers were homogenized in 10× volume/weight T-Per (Pierce) + PIs and fractionated by centrifugation at 1,000 × g, and the pellets were resuspended in 1 volume T-Per + 0.2% SDS, followed by sonication. Islets were prepared from disaggregated pancreata as described previously (Lawlor et al., 2006) and lysed in Tween lysis buffer, sonicated, and cleared by centrifugation at 12,000 × g prior to loading. For p19^{ARF} analysis, cell lysates were loaded on glycerol/acrylamide gels, fractionated by discontinuous electrophoresis, and electroblotted onto PVDF membranes. Anti-ERα (Santa Cruz, SC-543), anti-c-Myc (Santa Cruz, SC42 and 9E10), X-Myc1 (G.I.E.), and anti-p19^{ARF} 5-C3-1 (Bertwistle et al., 2004) were generously provided by M. Roussel (St. Jude Children's Research

Hospital, Memphis, TN, USA); anti-lamin A/C (Santa Cruz, SC7293) and anti-α-actin (Sigma) were used as primary antibodies. Secondary horseradish peroxidase-conjugated antibodies (Amersham) were detected by chemiluminescence.

Immunohistochemistry and Immunofluorescence

Paraffin-embedded sections (5 μm thick) were probed with Ki-67 antibody (NeoMarkers, SP6) used at 1:200 in 3% BSA overnight at 4°C and detected with biotinylated goat anti-rabbit (Vector Labs) followed by Vectastain ABC detection (Vector Labs) using stable diaminobenzidine (DAB) solution (Invitrogen). For BrdU/IdU double staining, mouse α-BrdU (1:20, Roche), which recognizes both BrdU and IdU, was used in conjunction with rat α-BrdU (1:200, Serotec), which recognizes BrdU only. Bound primary antibodies were detected using Alexa 488-conjugated α-mouse IgG and Alexa 568-conjugated α-rat IgG (Molecular Probes). For $p19^{ARF}$ immunohistochemistry, blocking was performed in 10% normal goat serum (NGS) with 0.1% Triton X-100. Primary antibody (5-C3-1) was diluted 1:10 in 3% NGS + 0.1% Triton X-100 and incubated overnight at 4°C. TUNEL staining was performed using an ApopTag peroxidase labeling kit (Chemicon) or an ApopTag fluorescein labeling kit (Chemicon) according to the manufacturer's directions. Otherwise, tissue sections were blocked overnight in 3% BSA prior to addition of peroxidase-conjugated anti-digoxigenin.

SUPPLEMENTAL DATA

The Supplemental Data include Supplemental Experimental Procedures, eight figures, and one table and can be found with this article online at http://www.cancercell.org/supplemental/S1535-6108(08)00367-X.

ACKNOWLEDGMENTS

We thank all members of the Evan laboratory for sage help in preparing this manuscript, most especially L. Soucek. Special thanks to F. Rostker for animal husbandry. We are grateful to M. Fried, M. McMahon, C. Broaddus, D. Hanahan, K. Shannon, D. Green, F. Mariani, D. Dankort, S. Schubbert, S. Oakes, J. Debnath, S. Kogan, and B. Weiss for insightful comments. We thank all members of the Cancer Center core facilities (N. Kileen, B. Hyun, K. Copren, L. Smythe, N. Korets, and E. Soliven). D.J.M. was supported in part by a Ruth L. Kirschstein NRSA Fellowship (CA099363). M.R.J. is Enrique Cepero Fellow of the Damon Runyon Cancer Research Foundation. This study was funded by NIH NCI grant R01-CA106526 to G.I.E.

Received: July 6, 2008
Revised: October 7, 2008
Accepted: October 31, 2008
Published: December 8, 2008

REFERENCES

Askew, D.S., Ashmun, R.A., Simmons, B.C., and Cleveland, J.L. (1991). Constitutive c-*myc* expression in an IL-3-dependent myeloid cell line suppresses cell cycle arrest and accelerates apoptosis. Oncogene *6*, 1915–1922.

Bertwistle, D., and Sherr, C.J. (2007). Regulation of the ARF tumor suppressor in *Eμ-Myc* transgenic mice: longitudinal study of Myc-induced lymphomagenesis. Blood *109*, 792–794.

Bertwistle, D., Zindy, F., Sherr, C.J., and Roussel, M.F. (2004). Monoclonal antibodies to the mouse p19(Arf) tumor suppressor protein. Hybrid. Hybridomics *23*, 293–300.

Bissonnette, R.P., Echeverri, F., Mahboubi, A., and Green, D.R. (1992). Apoptotic cell death induced by c-*myc* is inhibited by *bcl-2*. Nature *359*, 552–554.

Burns, K.A., and Kuan, C.Y. (2005). Low doses of bromo- and iododeoxyuridine produce near-saturation labeling of adult proliferative populations in the dentate gyrus. Eur. J. Neurosci. *21*, 803–807.

Chin, L., Schreiber-Agus, N., Pellicer, I., Chen, K., Lee, H.W., Dudast, M., Cordon-Cardo, C., and DePinho, R.A. (1995). Contrasting roles for Myc and Mad proteins in cellular growth and differentiation. Proc. Natl. Acad. Sci. USA *92*, 8488–8492.

Datta, A., Nag, A., Pan, W., Hay, N., Gartel, A.L., Colamonici, O., Mori, Y., and Raychaudhuri, P. (2004). Myc-ARF (alternate reading frame) interaction inhibits the functions of Myc. J. Biol. Chem. *279*, 36698–36707.

Eischen, C.M., Weber, J.D., Roussel, M.F., Sherr, C.J., and Cleveland, J.L. (1999). Disruption of the ARF-Mdm2-p53 tumor suppressor pathway in Myc-induced lymphomagenesis. Genes Dev. *13*, 2658–2669.

Evan, G., and Littlewood, T. (1998). A matter of life and cell death. Science *281*, 1317–1322.

Evan, G.I., Wyllie, A.H., Gilbert, C.S., Littlewood, T.D., Land, H., Brooks, M., Waters, C.M., Penn, L.Z., and Hancock, D.C. (1992). Induction of apoptosis in fibroblasts by c-myc protein. Cell *69*, 119–128.

Fanidi, A., Harrington, E.A., and Evan, G.I. (1992). Cooperative interaction between c-*myc* and *bcl-2* proto-oncogenes. Nature *359*, 554–556.

Fasbender, A., Lee, J.H., Walters, R.W., Moninger, T.O., Zabner, J., and Welsh, M.J. (1998). Incorporation of adenovirus in calcium phosphate precipitates enhances gene transfer to airway epithelia in vitro and in vivo. J. Clin. Invest. *102*, 184–193.

Fernandez, P.C., Frank, S.R., Wang, L., Schroeder, M., Liu, S., Greene, J., Cocito, A., and Amati, B. (2003). Genomic targets of the human c-Myc protein. Genes Dev. *17*, 1115–1129.

Finch, A., Prescott, J., Shchors, K., Hunt, A., Soucek, L., Dansen, T.B., Swigart, L.B., and Evan, G.I. (2006). Bcl-X_L gain of function and $p19^{ARF}$ loss of function cooperate oncogenically with Myc in vivo by distinct mechanisms. Cancer Cell *10*, 113–120.

Flinn, E.M., Busch, C.M.C., and Wright, A.P.H. (1998). myc boxes, which are conserved in myc family proteins, are signals for protein degradation via the proteasome. Mol. Cell. Biol. *18*, 5961–5969.

Harrington, E.A., Bennett, M.R., Fanidi, A., and Evan, G.I. (1994a). c-Myc-induced apoptosis in fibroblasts is inhibited by specific cytokines. EMBO J. *13*, 3286–3295.

Harrington, E.A., Fanidi, A., and Evan, G.I. (1994b). Oncogenes and cell death. Curr. Opin. Genet. Dev. *4*, 120–129.

Hermeking, H., and Eick, D. (1994). Mediation of c-Myc-induced apoptosis by p53. Science *265*, 2091–2093.

Indra, A.K., Warot, X., Brocard, J., Bornert, J.M., Xiao, J.H., Chambon, P., and Metzger, D. (1999). Temporally-controlled site-specific mutagenesis in the basal layer of the epidermis: comparison of the recombinase activity of the tamoxifen-inducible Cre-ER(T) and Cre-ER(T2) recombinases. Nucleic Acids Res. *27*, 4324–4327.

Jackson, E.L., Willis, N., Mercer, K., Bronson, R.T., Crowley, D., Montoya, R., Jacks, T., and Tuveson, D.A. (2001). Analysis of lung tumor initiation and progression using conditional expression of oncogenic K-*ras*. Genes Dev. *15*, 3243–3248.

Jackson, E.L., Olive, K.P., Tuveson, D.A., Bronson, R., Crowley, D., Brown, M., and Jacks, T. (2005). The differential effects of mutant p53 alleles on advanced murine lung cancer. Cancer Res. *65*, 10280–10288.

Johnson, L., Mercer, K., Greenbaum, D., Bronson, R.T., Crowley, D., Tuveson, D.A., and Jacks, T. (2001). Somatic activation of the K-*ras* oncogene causes early onset lung cancer in mice. Nature *410*, 1111–1116.

Juin, P., Hueber, A.O., Littlewood, T., and Evan, G. (1999). c-Myc-induced sensitization to apoptosis is mediated through cytochrome c release. Genes Dev. *13*, 1367–1381.

Juin, P., Hunt, A., Littlewood, T., Griffiths, B., Swigart, L.B., Korsmeyer, S., and Evan, G. (2002). c-Myc functionally cooperates with Bax to induce apoptosis. Mol. Cell. Biol. *22*, 6158–6169.

Kamijo, T., Weber, J.D., Zambetti, G., Zindy, F., Roussel, M.F., and Sherr, C.J. (1998). Functional and physical interactions of the ARF tumor suppressor with p53 and Mdm2. Proc. Natl. Acad. Sci. USA *95*, 8292–8297.

Kamijo, T., van de Kamp, E., Chong, M.J., Zindy, F., Diehl, J.A., Sherr, C.J., and McKinnon, P.J. (1999). Loss of the ARF tumor suppressor reverses premature replicative arrest but not radiation hypersensitivity arising from disabled ATM function. Cancer Res. *59*, 2464–2469.

Land, H., Parada, L.F., and Weinberg, R.A. (1983). Tumorigenic conversion of primary embryo fibroblasts requires at least two cooperating oncogenes. Nature *304*, 596–602.

Lawlor, E.R., Soucek, L., Brown-Swigart, L., Shchors, K., Bialucha, C.U., and Evan, G.I. (2006). Reversible kinetic analysis of Myc targets in vivo provides novel insights into Myc-mediated tumorigenesis. Cancer Res. *66*, 4591–4601.

Lewandoski, M., Wassarman, K.M., and Martin, G.R. (1997). *Zp3-cre*, a transgenic mouse line for the activation or inactivation of *loxP*-flanked target genes specifically in the female germ line. Curr. Biol. *7*, 148–151.

Littlewood, T.D., Hancock, D.C., Danielian, P.S., Parker, M.G., and Evan, G.I. (1995). A modified oestrogen receptor ligand-binding domain as an improved switch for the regulation of heterologous proteins. Nucleic Acids Res. *23*, 1686–1690.

Liu, J., and Levens, D. (2006). Making myc. Curr. Top. Microbiol. Immunol. *302*, 1–32.

Lowe, S.W., and Sherr, C.J. (2003). Tumor suppression by *Ink4a-Arf*: progress and puzzles. Curr. Opin. Genet. Dev. *13*, 77–83.

Lowe, S.W., Cepero, E., and Evan, G. (2004). Intrinsic tumour suppression. Nature *432*, 307–315.

Moore, J.P., Hancock, D.C., Littlewood, T.D., and Evan, G.I. (1987). A sensitive and quantitative enzyme-linked immunosorbence assay for the c-*myc* and N-*myc* oncoproteins. Oncogene Res. *2*, 65–80.

Nesbit, C.E., Tersak, J.M., and Prochownik, E.V. (1999). MYC oncogenes and human neoplastic disease. Oncogene *18*, 3004–3016.

Pelengaris, S., Khan, M., and Evan, G.I. (2002). Suppression of Myc-induced apoptosis in beta cells exposes multiple oncogenic properties of Myc and triggers carcinogenic progression. Cell *109*, 321–334.

Penn, L.J., Brooks, M.W., Laufer, E.M., and Land, H. (1990). Negative autoregulation of c-*myc* transcription. EMBO J. *9*, 1113–1121.

Popescu, N.C., and Zimonjic, D.B. (2002). Chromosome-mediated alterations of the MYC gene in human cancer. J. Cell. Mol. Med. *6*, 151–159.

Qi, Y., Gregory, M.A., Li, Z., Brousal, J.P., West, K., and Hann, S.R. (2004). p19ARF directly and differentially controls the functions of c-Myc independently of p53. Nature *431*, 712–717.

Queva, C., Hurlin, P.J., Foley, K.P., and Eisenman, R.N. (1998). Sequential expression of the MAD family of transcriptional repressors during differentiation and development. Oncogene *16*, 967–977.

Rabbitts, P.H., Watson, J.V., Lamond, A., Forster, A., Stinson, M.A., Evan, G., Fischer, W., Atherton, E., Sheppard, R., and Rabbitts, T.H. (1985). Metabolism of c-myc gene products: c-myc mRNA and protein expression in the cell cycle. EMBO J. *4*, 2009–2015.

Ramsay, G., Evan, G.I., and Bishop, J.M. (1984). The protein encoded by the human proto-oncogene c-*myc*. Proc. Natl. Acad. Sci. USA *81*, 7742–7746.

Sarkisian, C.J., Keister, B.A., Stairs, D.B., Boxer, R.B., Moody, S.E., and Chodosh, L.A. (2007). Dose-dependent oncogene-induced senescence *in vivo* and its evasion during mammary tumorigenesis. Nat. Cell Biol. *9*, 493–505.

Schmitt, C.A., McCurrach, M.E., de Stanchina, E., Wallace-Brodeur, R.R., and Lowe, S.W. (1999). *INK4a/ARF* mutations accelerate lymphomagenesis and promote chemoresistance by disabling p53. Genes Dev. *13*, 2670–2677.

Spencer, C.A., and Groudine, M. (1991). Control of c-*myc* regulation in normal and neoplastic cells. Adv. Cancer Res. *56*, 1–48.

Srinivas, S., Watanabe, T., Lin, C.S., William, C.M., Tanabe, Y., Jessell, T.M., and Costantini, F. (2001). Cre reporter strains produced by targeted insertion of EYFP and ECFP into the ROSA26 locus. BMC Dev. Biol. *1*, 4.

Tran, P.T., Fan, B.C., Bendapudi, P.K., Koh, S., Komatsubara, K., Chen, J., Horng, G., Bellovin, D.I., Giuriato, S., Wang, C.S., et al. (2008). Combined Inactivation of MYC and K-Ras oncogenes reverses tumorigenesis in lung adenocarcinomas and lymphomas. PLoS ONE *3*, e2125.

Vastrik, I., Kaipainen, A., Penttila, T.L., Lymboussakis, A., Alitalo, R., Parvinen, M., and Alitalo, K. (1995). Expression of the *mad* gene during cell differentiation in vivo and its inhibition of cell growth in vitro. J. Cell Biol. *128*, 1197–1208.

Wagner, A.J., Small, M.B., and Hay, N. (1993). Myc-mediated apoptosis is blocked by ectopic expression of *bcl-2*. Mol. Cell. Biol. *13*, 2432–2440.

Wagner, A.J., Kokontis, J.M., and Hay, N. (1994). Myc-mediated apoptosis requires wild-type p53 in a manner independent of cell cycle arrest and the ability of p53 to induce p21waf1/cip1. Genes Dev. *8*, 2817–2830.

Weber, J.D., Taylor, L.J., Roussel, M.F., Sherr, C.J., and Bar-Sagi, D. (1999). Nucleolar ARF sequesters Mdm2 and activates p53. Nat. Cell Biol. *1*, 20–26.

Zindy, F., Eischen, C.M., Randle, D.H., Kamijo, T., Cleveland, J.L., Sherr, C.J., and Roussel, M.F. (1998). Myc signaling via the ARF tumor suppressor regulates p53-dependent apoptosis and immortalization. Genes Dev. *12*, 2424–2433.